The TGF beta pathway is a key player for the endothelial-to-hematopoietic transition in the embryonic aorta

Lempereur, A.; Canto, P.Y.; Richard, C.; Martin, S.; Thalgott, J.; Raymond, K.; ... ; Jaffredo, T.

Developmental Biology 434 (2018) 292–303

Contents lists available at ScienceDirect

Developmental Biology

journal homepage: www.elsevier.com/locate/developmentalbiology

Evolution of developmental control mechanisms

The TGFβ pathway is a key player for the endothelial-to-hematopoietic transition in the embryonic aorta

A. Lempereur[a,1], P.Y. Canto[a,1], C. Richard[a], S. Martin[b,d], J. Thalgott[c], K. Raymond[c], F. Lebrin[b,c,d], C. Drevon[a], T. Jaffredo[a,*]

[a] Sorbonne Universités, UPMC Univ Paris 06, IBPS, CNRS UMR7622, Inserm U 1156, Laboratoire de Biologie du Développement, 75005 Paris, France
[b] CNRS UMR 7241/INSERM U1050, Center for Interdisciplinary Research in Biology, Collège de France, 11 Place Marcelin Berthelot, 75231 Paris CEDEX 05, France
[c] Einthoven Laboratory for Experimental Vascular Medicine, Department of Internal Medicine (Nephrology), Leiden University Medical Center, Leiden, The Netherlands
[d] MEMOLIFE Laboratory of Excellence and Paris Sciences et Lettres Research University, France

ARTICLE INFO

Keywords:
Hematopoieisis
Endothelium
Aorta
Embryo
Endothelial-to-hematopoietic transition
TGFß
Alk1
ES cells

ABSTRACT

The embryonic aorta produces hematopoietic stem and progenitor cells from a hemogenic endothelium localized in the aortic floor through an endothelial to hematopoietic transition. It has been long proposed that the Bone Morphogenetic Protein (BMP)/Transforming Growth Factor ß (TGFß) signaling pathway was implicated in aortic hematopoiesis but the very nature of the signal was unknown. Here, using thorough expression analysis of the BMP/TGFß signaling pathway members in the endothelial and hematopoietic compartments of the aorta at pre-hematopoietic and hematopoietic stages, we show that the TGFß pathway is preferentially balanced with a prominent role of Alk1/TgfßR2/Smad1 and 5 on both chicken and mouse species. Functional analysis using embryonic stem cells mutated for *Acvrl1* revealed an enhanced propensity to produce hematopoietic cells. Collectively, we reveal that TGFß through the Alk1/TgfßR2 receptor axis is acting on endothelial cells to produce hematopoiesis.

1. Introduction

Hematopoietic Stem and Progenitor Cells (HSPCs) are normally localized in the bone marrow where they are responsible for the life-long maintenance of the adult hematopoietic system. HSPCs are however produced early during development in the Aorta-Gonads-Mesonephros (AGM) region (Medvinsky and Dzierzak, 1996; Müller et al., 1994) from a specialized subset of endothelial cells (ECs) designated as hemogenic. HSPC production in the aorta is polarized to the aortic floor and appears as cell clusters thereafter referred as to Intra-Aortic Hematopoietic Clusters (IAHCs). In most vertebrate species, IAHCs lay in the aortic floor in close association with the endothelium. The only exception is the mouse wherein IAHCs are found both ventrally and dorsally although hematopoietic stem cells are restricted to the ventral part of the vessel (Taoudi and Medvinsky, 2007; Yokomizo and Dzierzak, 2010).

Cell-tracing experiments in chicken (Jaffredo et al., 2000, 1998) and mouse (Chen et al., 2009; de Bruijn et al., 2002; Sugiyama et al., 2003; Zovein et al., 2008) species indicate that IAHCs derive from hemogenic ECs through an Endothelial-to-Hematopoietic Transition (EHT). Time-lapse imaging techniques have documented this transition in mouse Embryonic Stem (ES) cells (Eilken et al., 2009; Lancrin et al., 2009) and have allowed to directly monitor HSPC formation in zebrafish (Bertrand et al., 2010; Kissa and Herbomel, 2010; Lam et al., 2010) and mouse embryos (Boisset et al., 2010) suggesting highly conserved mechanisms between species.

One of the key players for the hemogenic endothelium and IAHCs is the transcription factor Runx1. *Runx1* is expressed in IAHCs of mouse (North et al., 2002), *Xenopus* (Ciau-Uitz et al., 2000) zebrafish (Lam et al., 2010) and chicken (Richard et al., 2013) embryo and is required for their proper emergence (Chen et al., 2009; North et al., 1999) during EHT (Chen et al., 2009). Moreover, the use of ES cell cultures has also disclosed the critical role of *Runx1* for hematopoietic cell (HC) budding from the hemogenic endothelium (Lancrin et al., 2009). Recently, we reported that the sub-aortic mesenchyme is required *in vivo* to initiate *RUNX1* expression in hemogenic ECs and to allow emergence of IAHCs (Richard et al., 2013). Despite these advances, the molecular signal(s) triggering hematopoietic commitment and IAHC formation is yet to be defined.

* Corresponding author.
E-mail address: thierry.jaffredo@upmc.fr (T. Jaffredo).
[1] Equal contribution.

https://doi.org/10.1016/j.ydbio.2017.12.006
Received 11 October 2017; Received in revised form 7 December 2017; Accepted 8 December 2017
Available online 16 December 2017
0012-1606/

One potential signaling pathway controlling aortic hematopoiesis from hemogenic ECs is the BMP/TGFß axis. BMP4 has been found expressed in the subaortic mesenchyme in mouse (Durand et al., 2007), human (Marshall et al., 2000) and zebrafish (Wilkinson et al., 2009) and inhibition of BMP signaling was shown to decrease the number of aorta-associated HSPCs (Durand et al., 2007). A link between tgfß/bmp and runx1 has also been reported in *Xenopus*, (Walmsley et al., 2002). Both *Runx1* and the BMP/TGFß inhibitory protein Smad 6 (*SMAD6*) were shown to be transcriptionally regulated by BMP (Knezevic et al., 2011; Pimanda et al., 2007). TGFß1 is expressed by IAHCS during human development suggesting a role in embryonic hematopoiesis (Marshall et al., 2000). Recently, active TGFß signaling was shown to promote EC differentiation at the expense of HC in an ES cell differentiation model (Vargel et al., 2016) and to trigger hemogenic EC commitment and EHT in the developing zebrafish (Monteiro et al., 2016). Genetic studies in mouse and human have also provided strong evidence for a prominent role of TGFß signaling in normal and pathological EC function during vascular formation (Pardali et al., 2010). In particular TGFß was proposed to regulate the activation state of ECs between proliferation and quiescence (Goumans et al., 2002; Oh et al., 2000). In this context, VE-Cadherin has been reported to be a strong regulator of TGFß signaling linking the endothelial phenotype to the proper functioning of TGFß-associated receptors (Rudini et al., 2008). Of note, TGFß has also been assigned as one of the key players in Epithelial to Mesenchymal Transition (EMT), a mechanism involved in development, tissue repair and cancer (Kalluri and Weinberg, 2009; Lamouille et al., 2014), that closely resembles EHT (Goossens et al., 2011).

The TGFβ signaling pathway includes Bone morphogenetic proteins (BMPs), Growth and differentiation factors (GDFs), Anti-Müllerian Hormone (AMH), Activin, Nodal and TGFβ's, seven type I Activin-like kinase receptors (ALK1 to 7 also designated as ACVRL1, ACVR1, BMPR1A, ACVR1B, TGFßR1, BMPR1B and ACVR1C respectively), four type II serine-threonine kinase receptors (TGFβRII, BMPRII, ACTRIIA, ACTRIIB) and two type III receptors (Endoglin (Eng) and Betaglycan) (Supplementary Table 1) see also (Miyazono et al., 2010). Upon binding of one of the ligands to type II receptors, a specific type I receptor is recruited and activated by phosphorylation of a conserved amino acid sequence, the GS-domain. Phosphorylation of signaling molecules named Smads takes place in the cytoplasm. Phosphorylated Smads (P-Smads) associate with a co-Smad (Smad4) and migrate to the nucleus to regulate target genes. Classically, BMP receptor regulated-Smads (Smads1/5/8) are phosphorylated by the ACVRL1/ACVR1 group (ALK1/2) and BMPR1-group (ALK3/6) receptors, whereas TGFβ receptor-regulated-Smads (Smads2/3) are phosphorylated by the TGFβR1-group (ALK4/5/7) (Miyazono et al., 2010; Shi and Massague, 2003). However this Smad code is broken in ECs wherein TGFß-mediated proliferation and differentiation occur through a precise balance between ACVRL1 and TGFßRI signaling followed by the recruitment of R-SMADS 1–5 or R-SMADS 2–3 respectively (Goumans et al., 2002; Lebrin et al., 2004).

In the present study, we have investigated the BMP/TGFß signaling pathway in the context of aortic hematopoiesis using chicken and mouse species by studying the expression of 6 type I, 3 type II and 2 type III receptors, 7 ligands, and 8 Smads. Our data identified the TGFß pathway, in particular the type I and type II receptors, *Acvrl1* (*Alk1*) and *TgfßR2* respectively, as a hallmark of AGM ECs. Hematopoietic commitment decreased the expression of these two receptors and their associated Smad signaling in IAHCs. Importantly, ES cells heterozygous for *Acvrl1* (*Acvrl1*$^{+/-}$) displayed an enhanced propensity to generate HC. Collectively, our results will help better manipulating cells to produce hematopoiesis from ECs.

2. Material and methods

2.1. FACS sorting

Chicken eggs (Gallus gallus JA57 strain) were incubated at 38 ± 1 °C in a humidified atmosphere until the required stage. ECs were metabolically stained by inoculating Acetylated low-density lipoproteins-Alexa 488 into the heart of E2 or E3 embryos as described (Jaffredo et al., 1998; Richard et al., 2013; see Supplementary material and Section 2 for details). Cells from E9 embryos were stained with CD31-PE (BioLegend, clone MEC13.3 #102507) and CD45-FITC (BioLegend, clone 30-F11 #103107) antibodies, and AGM cells from E11.5 embryos with CD144-PE (BioLegend, clone BV13 #138009) and CD45-FITC. Both chicken and mouse embryo remnants were free of heart and digestive tract. After staining, cells were rinsed and sorted on MOFLO ASTRIOS (Beckman Coulter).

2.2. RNA extraction

RNA extraction was performed with RNeasy Mini Kit (Quiagen) according to the manufacturer's instructions. RNA was conserved at −80 °C, until reverse transcription.

2.3. Reverse transcription

DNA contamination was removed using DNAse (Ambion). Reverse transcription was performed according to Cloned AMV First-Strand cDNA Synthesis Kit (Invitrogen) for chicken RNA or to SuperScript III First-Strand Synthesis System (Invitrogen) for mouse RNA.

2.4. Quantitative Real-Time PCR

RNA was extracted and reverse transcribed as described above. Quantitative real time PCR was performed using FAM labeled TaqMan primers on Light Cycler 480 (Roche). All reactions were run in triplicates. Data were analyzed using relative quantification and the $2^{-\Delta\Delta Ct}$. Expression was quantified as fold change relative to *gapdh* and *18 s* RNA expression. Primers are described in Supplementary Table 2.

2.5. In situ Hybridization

For paraffin sections, embryos were fixed in 60% ethanol, 5% acetic acid and 30% formaldehyde (37% stock solution). After dehydration, they were embedded in Paraplast (Sigma) and cut at 7 µm. Hybridization was performed according to (Minko et al., 2003) and (Wilting et al., 1997).

2.6. RNA Probes

The following chick-specific riboprobes were used: *BMP4* was a gift from Dr M-A Teillet. *TGFβ2, TGFβ3* were gifts from Dr. D. Duprez and *SMAD6* from Dr. Neil Vargesson, Aberdeen University.

2.7. Immunostaining

Origins and dilutions of the antibodies used in the study are described in Supplementary Table 3. Of note, the anti-P-SMAD 2–3 was raised against P-SMAD2 but also recognized P-SMAD3 and was designated as anti-P-SMAD2-3 thereafter. The signal was amplified using the TSA kit, (NEN Life Science). Additional procedures and secondary antibodies can be found in the supplementary Material and Methods.

2.8. Embryonic Stem Cell lines (ES) culture

Acvrl1$^{+/+}$ and *Acvrl1*$^{+/-}$ ES cell lines were derived and cultured as described (Czechanski et al., 2014). ES cell lines were cultured in hanging drops to form EBs as described (Dang et al., 2002). Briefly, 1000 cells were cultured in 22 µl of GMEM supplemented with 20% FBS, 25 ng.ml^{-1} VEGF (450-32, Peprotech) and 50 ng ml^{-1} bFGF (450-33, Peprotech), hanging from the lid of the culture dish for 5 days

which allows the formation of cell aggregates. Subsequently, EBs were plated in 35 mm dish coated with 0.1% gelatin (G1393, Sigma) as described in medium composed of GMEM with 20% FBS, 25 ng ml^{-1} VEGF and 50 ng ml^{-1} bFGF, then cultured for 3, 5 or 7 days at 37 °C in 5% CO_2 atmosphere (Li et al., 2014).

3. Results

3.1. Patterns of BMPs, BMP antagonists and TGFßs during the aorta formation

We first examined the expression patterns of *BMP4* and 7 and of *TGFß1, 2* and *3* mRNAs by *in situ* hybridization (ISH) and immunohistology for BMP4 on cross sections at pre-hematopoietic (*BMP4*) and hematopoietic stages (BMP4, *TGFß2* and *3*) of chicken development with the aim to evaluate their association with the aorta microenvironment. For comparison, sections were performed at the wing bud level at the 13-somite stage (Hamburger and Hamilton (HH) stage 12) (Hamburger and Hamilton, 1951) when the embryo is still flat and the aortas paired, at the 20-somite stage (HH14) upon aortic fusion and at 3 days (HH19-20). *BMP7* mRNA was not found associated with the vessels in agreement with a previous report (Ahnfelt-Ronne et al., 2010) and was not investigated further. *BMP4* transcript was found in the dorsal part of the neural tube and the overlying ectoderm and in the lateral plate at the exception of the somite and the Wolffian duct (Fig. 1A) in keeping with previously published patterns (Reshef et al., 1998; Sela-Donenfeld and Kalcheim, 2002; Watanabe and Le Douarin, 1996). Around the aortic region, *BMP4* was present underneath the aortic anlage, in the splanchopleural mesoderm that will form the subaortic mesenchyme (Richard et al., 2013). A similar distribution was observed at the time of paired aorta fusion (Fig. 1B). Notably, *BMP4* mRNA was not expressed by the aortic endothelium.

At the hematopoietic stages, BMP4 protein was found associated with the sub-aortic mesenchyme and the mesonephros (Fig. 1C) in keeping with the pattern described for the mouse (Durand et al., 2007) and human (Marshall et al., 2000) embryo. Of note, the presence of BMP4 transcript was also detected in this region in the chicken embryo (our unpublished results and Huber et al. (2008)). *TGFß1* ISH did not give a readable pattern. However *TGFß2* and *3* were found in the aortic floor with *TGFß2* associated with the sub-aortic mesenchyme and the coelomic epithelium (Fig. 1D) and *TGFß3* around the aorta likely associated with the forming smooth muscle cells (Fig. 1E).

Taken together these patterns reveal that the sub-aortic mesenchyme is highly enriched with BMP4 and TGFß thus delineating a hematopoietic-promoting microenvironment.

3.2. Phosphorylated SMADs during the aorta formation

To gain insights into the cells that transduced the BMP/TGFß signal, we next examined the patterns of phosphorylated (P) SMAD1-5-8 associated with BMP and TGFß signaling and SMAD2-3 linked to TGFß signaling. SMADS were probed using specific antibodies directed against the P-SMAD complexes (see Material and Methods and Supplementary Material and Methods for antibody specificity). A high P-SMAD1-5-8 signal was found associated with the vessels at the earliest stages of vascular development (Fig. 2A, arrowheads). Coupling *BMP4* ISH to P-SMAD1-5-8 immunohistology revealed that *BMP4*-expressing cells did not co-localize with P-SMAD1-5-8 immunoreactive cells except in the dorsal part of the neural tube (compare Figs. 2A to 2B). At HH12, most of the P-SMAD1-5-8 positive cells were found associated with the aortic ECs, the dorsal aspect of the neural tube and the Wolffian duct (Fig. 2B). Immunodetection of P-SMAD2-3 at the nascent-mesoderm stage indicated the presence of numerous positive cells in the mesoderm, ectoderm and endoderm (Fig. 2C). At the paired aorta stage the P-SMAD2-3 signal was found in the ectoderm, endoderm and to a less extent, aortic ECs (Fig. 2D).

At the onset of aortic hematopoiesis, a P-SMAD1-5-8 signal was detected in cells scattered around the aorta and in the aortic endothelium that displayed the presence of the earliest $CD45^{+}$ cells (Fig. 2E). Of note, CD45, a hematopoietic-specific marker, expression

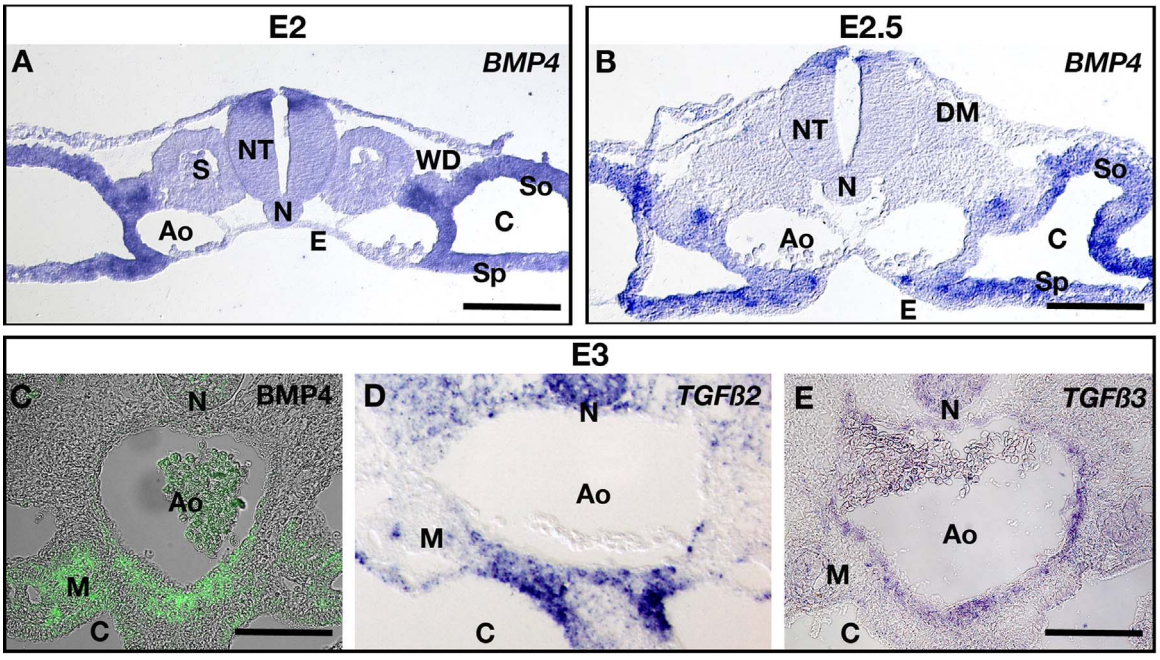

Fig. 1. *In situ* hybridization (ISH) and immunohistochemistry patterns of *BMP4, TGFß2 and 3* on sections of chicken embryos. HH12 (A), HH14 (B) and HH19-20 (C-E). Black frames indicate the respective ages on section. A. *BMP4* mRNA is expressed in the dorsal part of the neural tube, the overlying ectoderm and the lateral plate mesoderm. B. *BMP4* mRNA expression is present in the dorsal part of the neural tube and the lateral plate mesoderm. C. BMP4 protein expression follows the mRNA pattern (our unpublished results and Huber et al. (2008)). It is detected in the tissue immediately underneath the aorta and in the mesonephos. Erythrocytes in the aortic lumen display a strong background. Bar=70 µm. D. *TGFß2* mRNA is found enriched underneath the aorta and along the coelomic epithelium. E. *TGFß3* mRNA is associated with peri-endothelial cells. I-K scale bar=80 µm. Legend: Ao, aorta; C, coelom; DM, dermomyotome; E, endoderm; M, mesonephros; N, notochord; NT, neural tube; S, somite; So, somatopleural mesoderm; Sp, splanchnopleural mesoderm; WD, Wolffian duct.

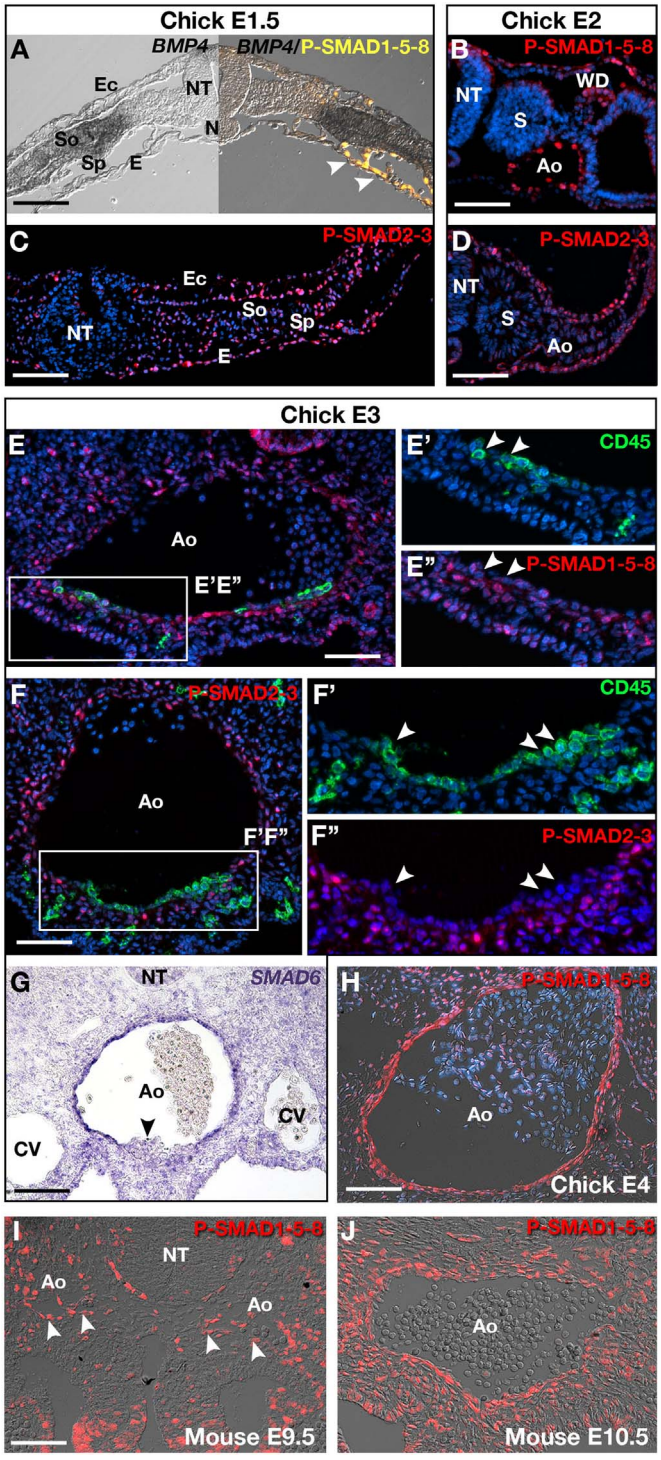

Fig. 2. Expression of phosphorylated (P) SMADS 1-5-8, 2–3 and the inhibitory SMAD6 at the level of the aorta. A-H chicken, I, J mouse. Identical embryonic stages are framed in black or indicated on individual pictures. A. Composite picture of a cross section showing *BMP4* ISH (left side) and *BMP4* ISH combined to immunofluorescence (IF) detection of p-SMADS 1-5-8 (right side) at the 10-somite stage immediately posterior to the last formed somites before formation of the aorta. Left. The BMP signal is prominent in the lateral plate (So + Sp) mesoderm, at the exception of the future somites, and the dorsal part of the neural tube. Right. The vessels associated with the splanchnopleural mesoderm display a high P-SMAD 1-5-8 signal localized to the cell nuclei (white arrowheads). The dorsal part of neural tube and some cells scattered in the ectoderm also display a visible signal. Of note, cells of the lateral plate express *BMP4* mRNA but did not express high levels of P-SMADS 1-5-8. Scale bar=200 µm. B. P-SMADS 1-5-8 IF at the early paired aorta stage (HH12) showing a strong signal in aortic ECs, Wolffian duct and peridermis. C-D. P-SMADS 2–3 IF. Posterior part of a 10 somite-stage chicken embryo. B-D scale Bar=50 µm. C. P-SMADS 2–3 IF signal is more widely distributed than that of the P-SMADS 1-5-8 being present in the ectoderm, mesoderm (including forming vessels) and endoderm at the notable expression of the newly formed neural tube. D. P-SMADS 2–3 IF is visible in the endoderm and ectoderm and to a less extent in aortic ECs (compare B to D). E-E". Combined immunodetection of P-SMADS 1-5-8 and CD45 at the initiation of hematopoeisis. E. Co-staining for CD45 antigen and P-SMADS 1-5-8. CD45 signal is present in a few cells undergoing EHT in the aortic floor. The P-SMADS 1-5-8 signal is present in both ECs and in some cells localized either immediately underneath the endothelial layer or scattered in the vicinity of the aorta. E'. Higher magnification of the frame in E showing CD45 expression in the aortic floor (white arrowheads). E". P-SMADS 1-5-8 expression is decreased in CD45 expressing cells (white arrowheads). F-F" Combined immunodetection of P-SMADS 2–3 and CD45 at the stage of hematopoietic clusters. F. P-SMADS 2–3 are present in ECs of the aorta and in cells localized immediately underneath the endothelial layer. F'. Higher magnification of the frame in F showing CD45 expression in the aortic floor. F". CD45-positive cells are negative for P-SMADS 2–3 expression (white arrowheads) E-F scale bar=100 µm. G. *SMAD 6* ISH at HH19, mid trunk level. The signal is present in the aortic endothelium but is absent from the large hematopoietic cluster present in the floor (arrowhead). Scale bar=100 µm. H. Cross section through the aorta at E4 i.e. post-hematopoietic, stage. P-SMADS 1-5-8 signal is present in the whole aortic endothelium and in the smooth muscle cells surrounding the vessel. Scale bar=150 µm. I-J. P-SMADS 1-5-8 IF in the prehematopoietic (I) and hematopoietic (J) aorta in the mouse embryo. Cross section. Distribution of P-SMADS is wider than in the chicken at similar embryonic stages. I. ECs of the aorta (Ao) are positive. Numerous cells of, likely, different origins also display a P-SMADS 1-5-8 signal. Arrowheads point out aortic ECs expressing P-SMADS 1-5-8. J. Aortic endothelium is stained. The tissues surrounding the aorta widely express P-SMADS 1-5-8 in keeping with (Zhang et al., 2014). I-J Scale bar=70 µm. Legend: Ec, ectoderm; CV, cardinal vein.

is accompanied by a progressive decrease of SMAD1-5-8 phosphorylation in HCs (compare Figs. 2E' to 2E"). A similar pattern was observed for P-SMAD2-3 although the signal was more widely distributed around the aorta than that of P-SMAD1-5-8 (Fig. 2F-F"). We also analyzed the pattern of *SMAD6* mRNA, an inhibitory SMAD, by ISH (Fig. 2G). Of note, *SMAD6* was found mostly restricted to the endothelium but was not present in the hematopoietic clusters in keeping with its inhibitory role on *Runx1* expression shown in the mouse model (Pimanda et al., 2007).

At the completion of hematopoiesis, the P-SMAD1-5-8 signal was detected in the endothelium and the immediately surrounding cells (Fig. 2H).

Finally, we completed the picture by analyzing the P-smad1-5-8 during mouse development. At E9.5, P-SMAD1-5-8 was detected in ECs of the paired aorta and some cells scattered in the mesenchyme (Fig. 2I). At E10.5, P-smad1-5-8 was widely distributed in the aortic region in keeping with a previously published report (Zhang et al., 2014), not only in ECs but also in cells surrounding the aorta (Fig. 2J).

In conclusion P-SMAD1-5-8 and to a lesser extent, P-SMAD2-3 phosphorylation is a hallmark of ECs from the onset of vascular formation. During EHT and the subsequent emergence of IHACs, P-SMAD1-5-8 and P-SMAD2-3 expression decreased on HCs indicating a down-regulation of the BMP/TGFß pathway. They however remained expressed by ECs and by cells of the surrounding mesenchyme.

3.3. Revealing BMP signaling with a transgenic mouse to monitor the transcriptional activity of Smad1-5

We used the transgenic mouse line BRE:*gfp* reporting P-SMAD1-5 activity through the *Id1* promoter (Monteiro et al., 2008) to reveal cells transducing the BMP/TGFß pathway. We analyzed pre-hematopoietic and hematopoietic stages for GFP expression and, when useful, co-detected the GFP signal with the expression of CD31, an endo-hematopoietic marker. In whole mounts, the GFP signal was strongly present in the limb bud, embryonic liver and segmental arteries (Supplementary Fig. 1A). On section, following fixation and GFP staining using an anti GFP antibody followed by tyramide signal amplification (see Section 2 and Supplementary Table 2 for details), GFP was present in the aorta, associated with ECs and in small vessels around the neural tube and the intestine (Supplementary Fig. 1B) at the exception of the cardinal veins. A closer view of the aorta revealed an ensemble of high and low GFP-expressing cells associated with the endothelium (Supplementary Fig. 1C) in keeping with a previous report (Crisan et al., 2015). Co-staining with CD31 identified several budding cells with overlapping signals (Supplementary Fig. 1D, E). Using the same mouse model, it was recently shown that all hematopoietic stem cells reside in the GFP^+ fraction when cells are isolated *in vivo* from E11.5 embryos (Crisan et al., 2015) whereas hematopoietic stem cells were distributed in both the GFP^+ and GFP^- fractions when cells were isolated after a culture period of 3 days (Crisan et al., 2016). Since it was not completely clear whether the mouse line reported either BMP or TGFß activity (James et al., 2010; Liang et al., 2009) or both, we decided to employ a flow cytometry sorting strategy followed by real-time quantitative PCR (RT-qPCR) to analyze the BMP/TGFß pathway.

3.4. Quantitative PCR analysis of the BMP/TGFβ signaling components in ECs and IHACs at the pre-hematopoietic and hematopoietic stages of chicken and mouse AGM

Since P-Smad1-5-8 and 2–3 decreased in aortic clusters, we decided to further characterize the expression of the BMP/TGFß signaling components in ECs and in HC using RT-qPCR with a collection of TaqMan probes (Supplementary Table 2) at the pre-hematopoietic and hematopoietic stages of the AGM in both chicken and mouse embryos. At pre-hematopoietic stages, AGM ECs were sorted based on the expression of endothelial-specific markers and the exclusion of CD45 expression. For the chicken, E2 and E3 embryos were used. ECs were stained following intra-cardiac inoculation of human Ac-LDL coupled to Alexa fluor 488 (AF488-Ac-LDL, Molecular probes). For the mouse, embryos of 20–22 somite pairs i.e., early E9.5 were used. Anti-CD31 (Pecam-1) antibody was chosen to identify ECs. A mean of 32–37 and 45–47 somite pairs were used to select E10.5 and E11.5 embryos respectively. Anti VE-Cadherin (CDH5, CD144) and CD45 antibodies were used to select EC and HC respectively. The IAHC population was validated for the combined expression of *CDH5* and *PTPRC* (CD45) as already reported (Richard et al., 2013). The double negative population (i.e. the embryo remnants) was retained as a baseline of expression. Accuracy of the sorting was verified with *VE-cadherin* and *RUNX1* as respectively EC-specific and hemogenic EC-specific genes for the endothelial fraction (not shown). The plots are displayed in Supplementary Fig. 2.

For the chicken at the pre-hematopoietic stage, type I receptor expression was characterized by a strong expression of *ACVRL1* (*ALK1*), a weaker but significant expression of *ACVR1* (*ALK2*) and a low expression of *BMPR1B* (*ALK6*) in ECs. The other type I receptors *BMPR1A* (*ALK3*) and *ACVR1B* (*ALK4*) were not significantly expressed compared to the negative cell fraction (Fig. 3A). A strong expression of *TGFβR2* and a weaker but significant expression of *BMPR2* distinguished the expression of the type II receptors (Fig. 3B). Type III receptor expression was characterized by a strong presence of *ENG (ENDOGLIN)* and a weaker expression of *TGFβR3 (BETAGLYCAN)* (Fig. 3C). Concerning the ligands, *BMP4* was weakly expressed in ECs compared to the rest of the AGM tissues whereas *BMP9* and *10* were not detected at this stage in this tissue (not shown). *TGFβ2* was not analyzed in the chicken embryo because no efficient qRT-PCR probe could be generated and *TGFβ1* and *3* did not display a statistically significant signal in ECs. In contrast, *BMP4* was significantly down-regulated in ECs (Fig. 3D). We also analyzed the expression of *SMADs*1–8 mRNAs with a special focus in non-phosphorylated SMADs i.e., *SMAD4, 6, 7*. For the chicken, no probe for *SMAD7* was found but *SMAD6*, an inhibitory SMAD, displayed a significantly increased expression (Fig. 3E) consistent with the ISH pattern (Fig. 2G).

A similarly consistent pattern was found in the mouse AGM for *Acvrl1*, *Acvr1* and *Bmpr1b* as type I receptors, *Tgfβr2* as type II receptors and *Eng* and *Tgfβr3* as type III receptors indicating the presence of conserved mechanisms (Fig. 3F-J). However *Bmpr1a* as type I, *Bmpr2* and *Acvr2a* as type II receptors displayed a different pattern between the two species. *Tgfβ1* and *Tgfβ3* displayed a significant increase not revealed for the chicken. *Tgfβ2* was not significantly expressed in ECs (Fig. 3I) in keeping with its specific role in heart development (Wagner and Siddiqui, 2009). Neither *Bmp2*, *Bmp9* nor *Bmp10* were detected at this stage in agreement with the results on the chicken embryo (not shown). *Smad6,* and to a lesser extent *Smad7,* were found increased in the EC fraction (Fig. 3J). Collectively, the strong presence of *Acvrl1* and *TgfβR2* as type I and II receptors respectively indicates that the TGFß pathway acts predominantly in ECs at the pre-hematopoietic stage and is likely using a TGFß1 autocrine loop, at least in the mouse species. This receptor make up is consistent with the expression of P-Smad1-5 in ECs. Since the antibody we used on section recognized equally P-Smad1-5-8 and P-Smad1-5 complexes, the prevalence of the TGFß pathway in ECs was likely.

We next analyzed the expression of the BMP/TGFß pathway in ECs and IHACs on chick E3 and mouse E11.5 AGM respectively, the developmental stages where HSPCs were detected (Dzierzak and Speck, 2008; Medvinsky et al., 2011). The same sorting strategy was used except that VE-cadherin (CD144) replaced CD31 as endothelial-specific marker for the mouse species. The co-expression of either human AcLDL-DiI or CD144 and an intermediate level of CD45 ($CD45^{int}$) authenticating hematopoietic progenitors was used to isolate IAHCs as reported (Richard et al., 2013). The double-negative population served as baseline for RT-qPCR. The TGFß-oriented pattern found at the pre-hematopoietic stage did not vary significantly for ECs between the pre-hematopoietic and hematopoietic stages. The hematopoietic fraction was characterized by a significant decrease of *Acvrl1* (Fig. 4A, F) *and Eng* (Fig. 4C, H) in both species and a significant decrease of *TGFβR2* for the chicken and a tendency to decrease for the mouse (Fig. 4B, G). *TGFβR3* expression also significantly varied between the two fractions for the chick but not for the mouse. *TGFβ1*, *2* and *3* ligands were detected but not significantly differentially expressed. This was also the case for *BMP4* (Fig. 4D, I). A strong decrease of *SMAD6* was observed in the IHAC fraction for the chicken (Fig. 4E) whereas the mouse IHAC fraction displayed a slightly higher level of Smad6 than the EC fraction (Fig. 4J).

Taken together our results confirmed the prominent expression of the TGFß pathway through *Acvrl1* (*Alk1*) and *TgfβR2* as a hallmark of ECs. Our data also revealed a downgrading of *Acvrl1* and *TgfβR2* along hematopoietic commitment and, contrary to expectations, underlined the unbalanced pattern for the BMP pathway in AGM hematopoietic cells.

We performed the same analysis on E10.5 (32–37 somite pairs) mouse embryos, the time when EHT occurs (Swiers et al., 2013) and HSPC production reaches a maximum (Yokomizo and Dzierzak, 2010). Interestingly, EC and IHAC fractions displayed a similar pattern

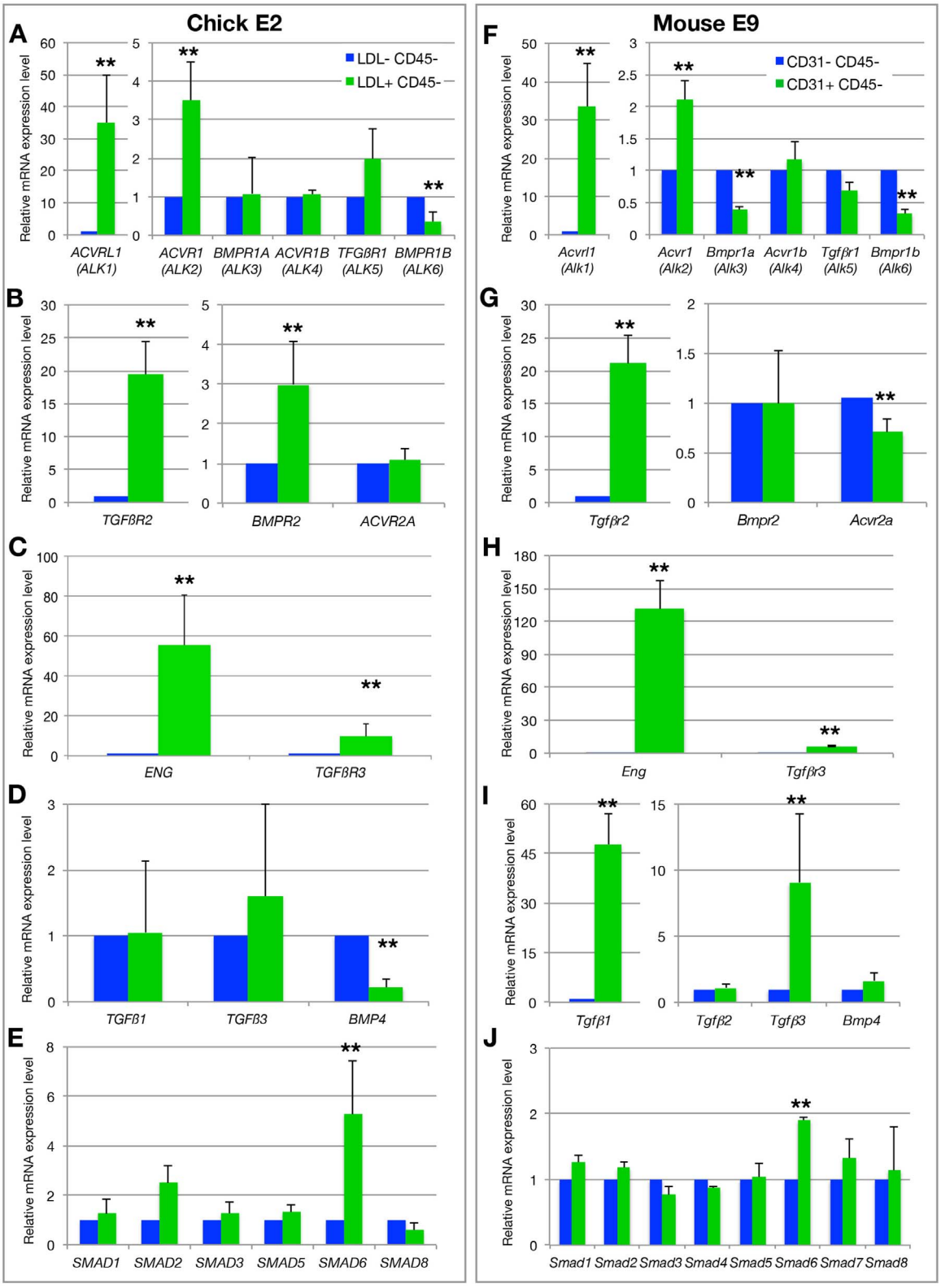

Fig. 3. RT-qPCR analysis of the BMP/TGFß pathway in AGM ECs at the pre-hematopoietic stage in chicken (A-E) and mouse (F-J) embryos, i.e., E2.5 and early E9.5 (20–22 somite pairs), respectively. ECs (green) were sorted on the basis of AcLDL uptake (chicken) and CD31 expression (mouse) and the exclusion of CD45 expression. The double negative cell fraction serves as reference. Relative expression of mRNAs ($2^{-\Delta\Delta Ct}$). A, F. Type I receptors; B, G. Type II receptors; C, H. Type III receptors; D, I. ligands; E, J. Smads. The error bars represent SEM. ***p < 0.01, **p < 0.25, *p < 0.5.

(Supplementary Fig. 3) indicating that regarding the BMP/TGFß pathway, the two cell populations are close to one another. This should be compared to the pattern found at E11.5 wherein the contrast between ECs and IHACs is more pronounced.

3.5. Acvrl1 (Alk1) is down regulated in IAHCs

Given the importance of *Acvrl1* in hematopoietic production, we decided to focus on this receptor in the aorta of both chicken and mouse

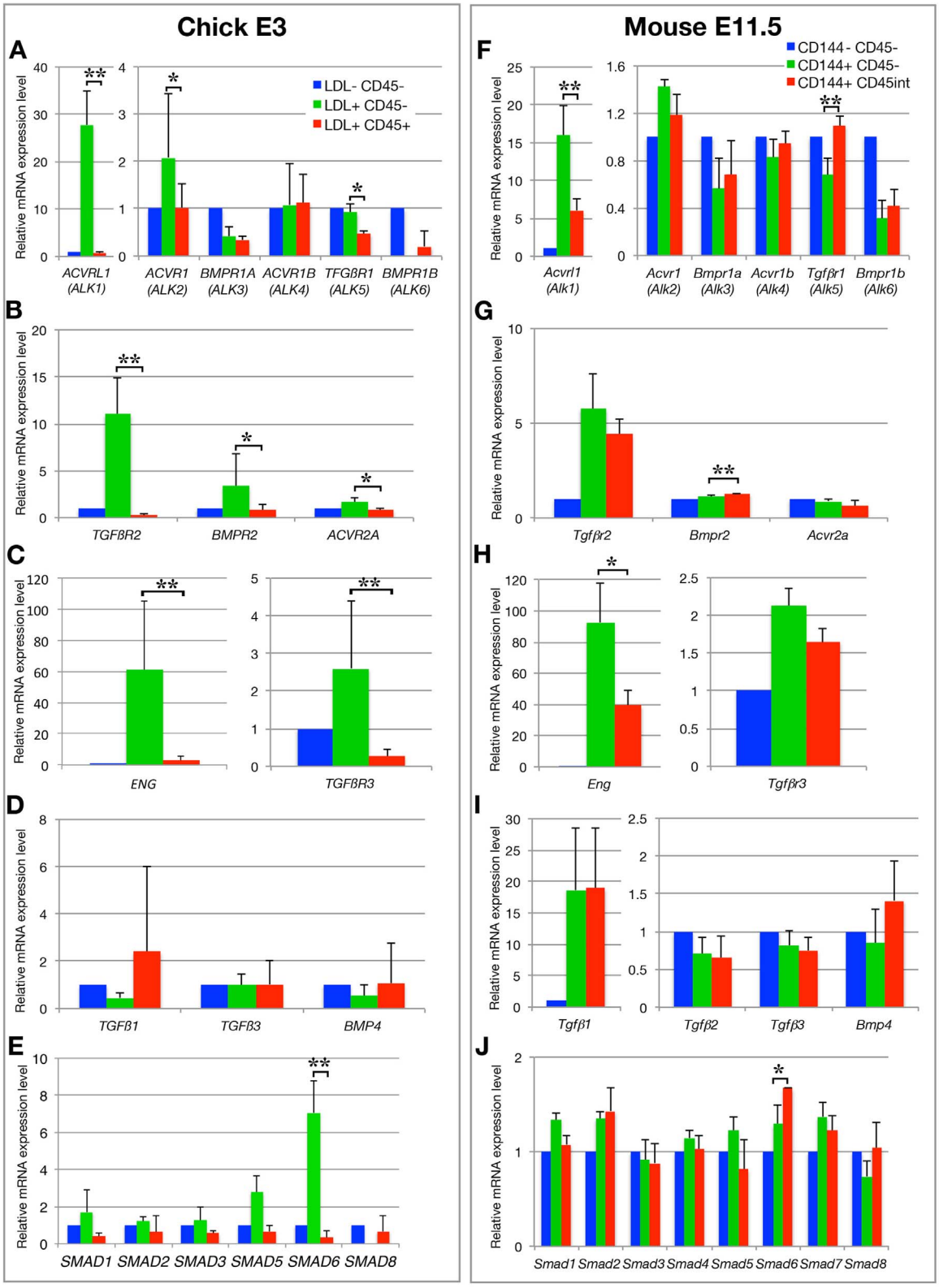

Fig. 4. RT-qPCR analysis of the BMP/TGFß pathway in AGM ECs and HCs at the hematopoietic stage in chicken (A-E) and mouse (F-J) embryos, i.e., E3.5 and E11.5, respectively. ECs (green) were sorted on the basis of AcLDL uptake (chicken) and CD144 expression (mouse) and the exclusion of CD45 expression. The hematopoietic cell cluster fraction (red) was sorted on the basis of the expression of AcLDL uptake (chicken) and CD144 (mouse) and the expression of $CD45^{intermediate}$. The double negative cell fraction serves as reference. Relative expression of mRNAs ($2^{-\Delta\Delta Ct}$). A, F. Type I receptors; B, G. Type II receptors; C, H. Type III receptors; D, I. ligands; E, J. Smads. The error bars represent SEM. ***p < 0.01, **p < 0.25, *p < 0.5.

species. At the time this study was initiated, no *ACVRL1* cDNA sequence was clearly assigned for the chicken species. Comparison of Ensemble and NCBI databases allowed isolating a cDNA with a strong homology to mammalian and non-mammalian *Acvrl1* transcripts (Fig. 5A and Supplementary Results for details). The resulting open reading frame encoded a putative protein of 498 amino acids containing an activin receptor domain, a TGFß GS domain and a protein kinase domain (Fig. 5B), in keeping with the global organization of the receptor.

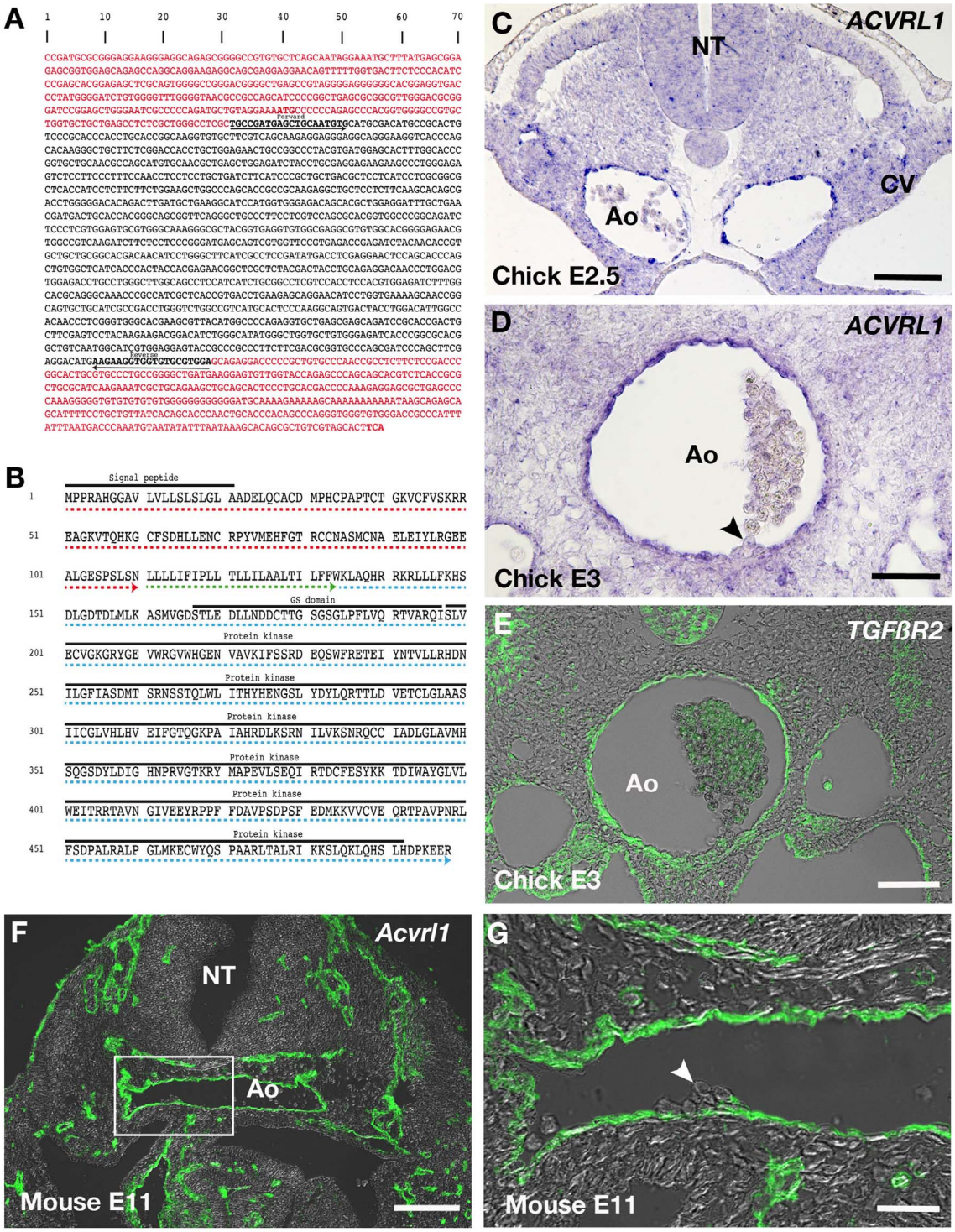

Fig. 5. Chicken *ACVRL1* cDNA sequence, protein domains and mRNA expression on chicken embryo section and expression pattern on mouse aorta section. A. Predicted cDNA sequence of the chicken Acvrl1 gene retrieved from the NCBI database (XM_015300268.1). In black, the cloned cDNA used to synthesize the chicken ISH probe. Start and Stop codons are in bold. Positions of the forward (direct) and reverse (complementary) primers are indicated. B. Chicken ACVRL1 protein and putative functional domains. Red: extracellular, green: transmembrane, blue: intracellular. C-D *ACVRL1* mRNA expression by ISH on sections at prehematopoietic E2.5 (C) and hematopoietic E3 (D) stages. scale bar=70 µm. *ACVRL1* mRNA is expressed in ECs of the aorta but not expressed in IAHCS (arrowhead). Scale bar=100 µm. G. Immunodetection of TGFßRII on section. E3 chicken embryo. Scale bar=90 µm E-F. Immunodetection of *Acvrl1* on section of E11.5 aorta of mouse embryo. F. *Acvrl1* is present in ECs of most vessels. Scale bar=80 µm. G. Expression is lost in IAHCS (arrowhead). Scale bar= 30 µm.

We next synthetized an *ACVRL1* probe (Fig. 5A) and performed *in situ* hybridization on chicken embryo section at the time of paired aorta and aortic hematopoiesis respectively. *ACVRL1* signal was restricted to the endothelial tree being present in the aorta, cardinal veins and smaller vessels scattered throughout the embryo (Fig. 5C, D). It was found down-regulated in IAHCs (Fig. 5D) in keeping with the differential expression revealed by RT-qPCR. Of note *TGFßR2*, the only type II receptor for TGFß, was found enriched in ECs and in the mesonephros region in the chicken embryo (Fig. 5E).

Immunostaining performed on the E11.5 mouse embryo using an ACVRL1-specific antibody revealed expression in most of the vascular ECs (Fig. 5F) but an absence on IAHCs (Fig. 5G).

3.6. Acvrl1 haplo insufficiency promotes hematopoietic production from cultured embryoid bodies

To gain insights into the role of Acvrl1 and the TGFß axis in EHT and hematopoiesis, we compared Wild-Type (WT) to *Acvrl1* heterozygous (*Acvrl1*$^{+/-}$) mouse ES cells for their capacity to produce endothelial and hematopoietic cells from ES cell-derived embryoid bodies (EBs). The differentiation of ES cells into EBs is a powerful method to explore the cellular and molecular mechanisms that regulate embryonic hematopoiesis. WT (IB10 or Thalk1-1 clones) and *Acvrl1*$^{+/-}$ (A60-3, A60-2 or Thalk 1–6 clones) EBs were followed over a period of 12 days and checked regularly for the presence of round cells. The first conspicuous production of round, floating cells was observed around day 7 and was particularly visible at day 12 around *Acvrl1*$^{+/-}$ flat cell colonies whereas few or no round cells were found in the WT colonies (Fig. 6A, B). Floating cluster-forming cells were visible in the culture supernatant of *Acvrl1*$^{+/-}$ EBs (Fig. 6C). We performed FACS analysis using isolated cells from WT and *Acvrl1*$^{+/-}$ EBs at day 12 using CD45 and CD144, this latter used as endothelial-specific marker. *Acvrl1*$^{+/-}$ cells produced significantly more (1.79 fold, n=3) hematopoietic cells than their WT counterparts (Fig. 6D); a ratio confirmed (1.3 fold, n=2) when a time course analysis was performed (Fig. 6E). The percentage of ECs did not however significantly vary between WT and *Acvrl1*$^{+/-}$ cells (not shown). Increased formation of CD45^{+} cells was further confirmed on immunohistological analysis of sections of day 12 wt and *Acvrl1*$^{+/-}$ EBs using CD45 and CD144 co-immunostainings. WT EBs displayed CD144 staining and a low CD45 signal (Fig. 6F). In contrast, *Acvrl1*$^{+/-}$ EBs showed a strong propensity to express CD45 confirming the data obtained by flow cytometry (Fig. 6G). Taken together these results indicate that the level of Avcrl1 influenced the endothelial to hematopoietic balance in an *ex vivo* ES differentiation assay in keeping with the data obtained on the embryonic aorta.

4. Discussion

Using an ensemble of gene expression patterns, RT-qPCR on purified cell populations and a functional assay using ES cells, we disclose the critical role of the TGFß pathway through the Alk1-TgfßR2-Smads1-5 axis to control EHT and hematopoietic production in the embryonic aorta.

The BMP pathway has long been considered as a main actor in blood formation. Ventral mesoderm, endothelial and hematopoietic precursors are induced by BMP4 and inhibited when BMP4 signaling is impaired (Maeno et al., 1996). In addition, BMP4 has also been shown to enhance stem cell activity during *ex vivo* culture of human cord blood cells (Bhatia et al., 1999) and hematopoietic differentiation of human ES cells (Chadwick et al., 2003). The prominent presence of BMP4 in the sub-aortic mesenchyme even reinforce this idea, suggestive of a major role for BMP4 in aortic hematopoiesis (Marshall et al., 2000; Durand et al., 2007; Wilkinson et al., 2009) and HSC maintenance (Durand et al., 2007). We indeed find BMP4 expressed in the lateral plate mesoderm at the somitic stages and underneath the aorta during aortic hematopoiesis, but the make up of BMP/TGFß type I and II receptors in ECs and in emerging hematopoietic cells is not fully consistent with its prominent role in aorta-associated hematopoiesis. Interestingly, *TGFß2* expression is polarized underneath the aorta suggesting its possible role in EHT and aortic hematopoiesis. P-SMAD1-5-8 are expressed in ECs at early stages of development in line with a previous work (Faure et al., 2002). However the P-SMAD1-5-8 pattern at these early stages is not totally compatible with the BMP4 mRNA distribution found in the lateral plate. This discrepancy may be attributed to a diffusion of active BMP4 to the endothelium or the existence of other TGFß/BMP ligands utilizing the same SMAD code for signal transduction. *BMP9* and *BMP10*, two other members of the BMP family are known to play a role in vascular quiescence (David et al., 2008) and vascular versus lymphatic EC specification (Kume, 2010) through activation of P-SMAD1-5-8. However none of these were detected at the stages examined using the sensitive RT-qPCR method ruling out an early role of these two factors on the endothelium.

In addition to BMPs, P-SMAD1-5, but not 8, signaling is also used by the TGFß pathway through the Alk1-Tgfßr2 axis (Lebrin et al., 2005). P-SMAD2-3 is found in ECs but also detected in other cell types suggesting a more pleiotropic role. It is known that EC migration and proliferation are regulated by two distinct TGFß signaling cascades namely Alk1-Tgfßr2-P-SMAD1-5-8 and Alk5-TgfßR2-P-SMAD2-3 responsible respectively, for activation and inhibition of EC migration and proliferation depending on the local concentrations of TGFß (Goumans et al., 2002). The presence of Endoglin suggests a bias towards Alk1 and Smad1/5 signaling at the expense of Alk5-Psmad2-3 (Finnson et al., 2010). VE-cadherin, which promotes EC-EC adherens junctions acts as a critical regulator of type I and II receptor complex assembly (Rudini et al., 2008). The joint presence of P-smad1-5-8 and 2–3 and of Alk1 and Alk5 may argue for a balanced role of these two receptors in aortic ECs with a more prominent role of Alk1 during the activated EC state at these embryonic stages. The fine tuned control of the EC status is even reinforced by the presence of the inhibitory Smad6 in aortic ECs in line with a control of Runx1 expression in mice (Pimanda et al., 2007). In conclusion the prominent expression of Alk1-Tgfßr2-Endoglin-P-Smad1-5-8 and to a lesser extent of Alk5-TgfßR2-P-Smad2-3 is a hallmark of aortic ECs before hematopoiesis.

Initiation of aortic hematopoiesis and IAHC formation is accompanied by a significant decrease of both the TgfßRII-Acvrl1-Endoglin-P-Smad1-5-8 axis and the TgfßRII-TgfßRI-P-Smad2-3 axis indicating a global down-regulation of the pathway as hematopoietic program is initiated. This down-regulation is completely in keeping with a decrease of the endothelial identity during EHT associated with the loss of VE-Cadherin mRNA expression and the gain of *PU1* and *C-MYB* transcription factors (Richard et al., 2013). The highly similar endothelial and hematopoietic patterns found in the mouse at E10.5 and the very balanced pattern found at E11.5 is fully in keeping with the model proposed by De Bruijn and colleagues who report a progressive loss of endothelial potential by the hemogenic endothelial cell fraction and an early onset of hematopoietic-specific genes (Swiers et al., 2013). In Swiers et al., the endo-hematopoietic balance is complete at E10.5. Using our gene set, we disclose a complete endo-hematopoietic switch slightly later at E11.5 but used a somewhat different combination of markers with VE-Cadherin and CD45^{int} expression that may explain the discrepancy. *Smad6* an inhibitor of BMP/TGFß signaling, is down-regulated in IAHC as revealed by *in situ* hybridization and RT-qPCR. This is in keeping with a proposed feedback loop in which Smad6 inhibits Runx1 by mediating its degradation by the proteasome (Pimanda et al., 2007).

In addition to its physiological role in developing ECs, TGFß signaling is also implicated in EMT that turns epithelial cells into mobile mesenchymal cells, a mechanism integral to development but also to wound healing and cancer (Lamouille et al., 2014). Interestingly, ECs can transdifferentiate into a mesenchymal cell/stem cell phenotype, a process known as EndMT developmentally required for the formation of endocardial cushions and involved in fibroblast accumulation in mouse models of renal, pulmonary and cardiac fibrosis (Medici and Kalluri, 2012; van Meeteren and ten Dijke, 2012). EndMT is characterized by the down-regulation of the junction-specific molecules VE-Cadherin, CD31 and Claudin-5 through the expression of the transcription factor Snail and is induced by either TGFß2 or BMP4. EMT and EndMT are indeed reminiscent of EHT since EndMT results in the activation of a mesenchymal cell and stem cell program and EHT into the activation of hematopoietic cell and HSC program. Whether EndMT and EHT employ similar if not identical molecular mechanisms is not known but is likely. Our recent results indicate that the sub-aortic mesenchyme plays a key role in the initiation of Runx1 expression and hematopoietic emergence (Richard et al., 2013). To

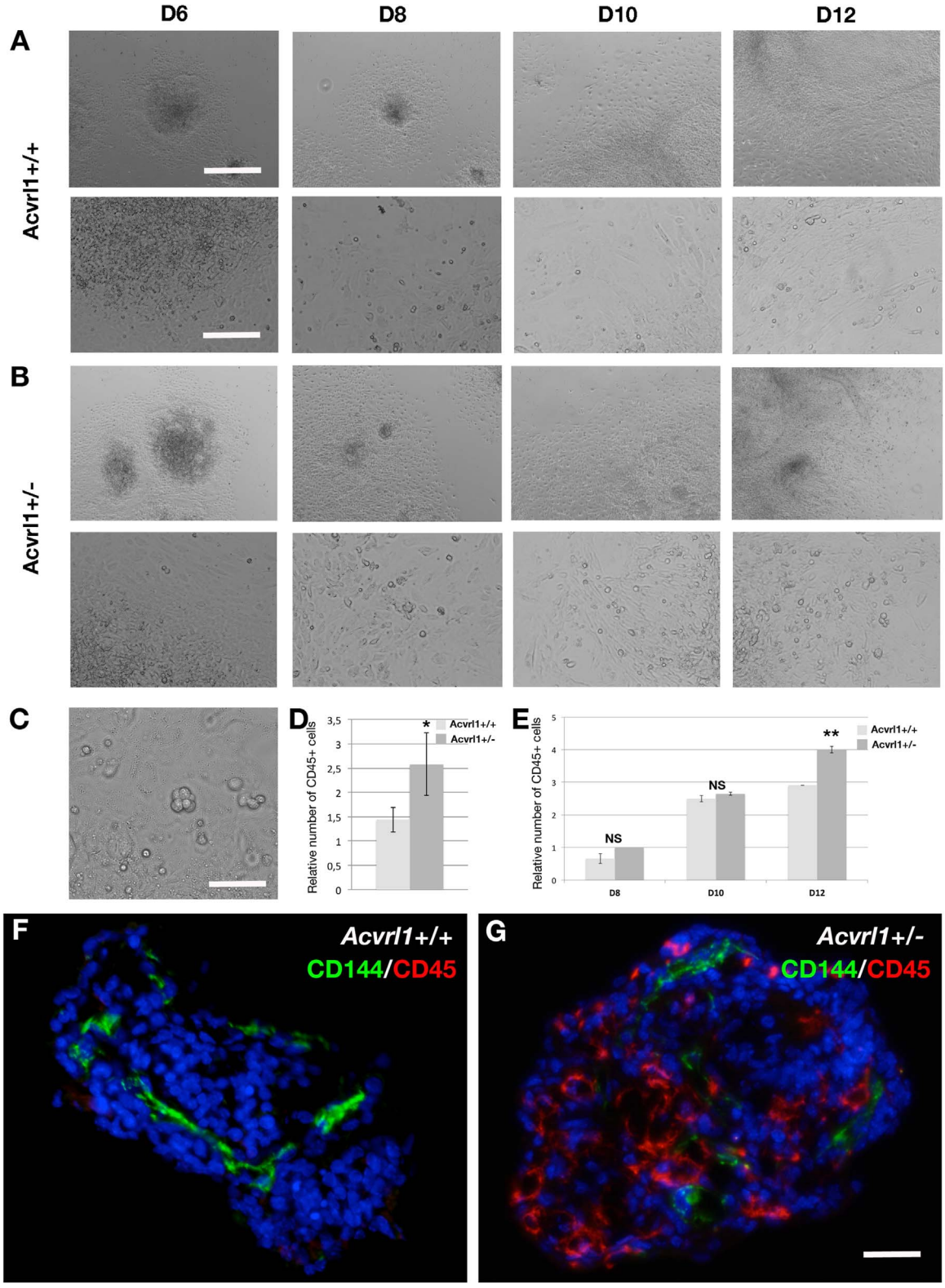

Fig. 6. Hematopoietic and endothelial production in WT *Acvrl1*$^{+/+}$ and *Acvrl1*$^{+/-}$ embryoid bodies. A-B. representative images culture of embryoid body colonies of WT (A) or Acvrl1$^{+/-}$ (B) at 6, 8, 10 and 12 days of culture. Note the increasing number of round cells in the *Acvrl1*$^{+/-}$ condition. C High magnification of round cell clusters at day 12 of *Acvrl1*$^{+/-}$ culture of embryoid bodies. D, E. Comparison by flow cytometry analysis between *Acvrl1*$^{+/+}$ and *Acvrl1*$^{+/-}$ CD45^{+} hematopoietic cells produced at day 12 (D) and a follow up at day 8, 10, 12 (E) of culture of embryoid bodies. F, G. Immunohistological analysis of CD144 (green) and CD45 (red) on sections of *Acvrl1*$^{+/+}$ (F) and *Acvrl1*$^{+/-}$ (G) embryoid bodies. Scale bar=15 µm.

understand the mechanism by which the sub-aortic mesenchyme informs ECs awaits further investigation.

Experiments using EBs differentiated from *Acvrl1*$^{+/-}$ mouse ES cells suggest a bias towards the hematopoietic lineage. This is in keeping with a specific requirement for Alk1 in EHT and early hematopoietic commitment that we disclose using gene expression studies. This also indicates that, in addition to its role in EC homeostasis, Acvrl1 plays a pivotal role in the EC versus hematopoietic cell commitment/differentiation.

Taken together, we unveil here the requirement for TGFß signaling

to control EHT and hematopoietic commitment *in vivo and ex vivo*. Identification of the spatial and temporal requirements will be instrumental for the future generation of hemogenic endothelium and hematopoietic production *ex vivo* from various cellular sources for therapeutic purposes.

Acknowledgments

We thank Dr. D. Duprez for help in obtaining the TGFß pattern on section. We are grateful to the IBPS RT-qPCR platform and Centre de Recherche St Antoine flow cytometry platform (A-M Faussat). We also thank Sophie Gournet (UMR CNRS 7622) for excellent photographic assistance. This study was supported by grants from the Agence Nationale de la Recherche (ANR-14-OHRI-0011-01), Association pour la Recherche sur le Cancer (20141201965) and Association Maladie Rendu Osler for FL and from the Fondation pour la Recherche Médicale (DEQ20100318258) and from the Agence Nationale pour la Recherche/California Institute for Regenerative Medicine (ANR/CIRM 0001-02) for TJ.

Appendix A. Supporting information

Supplementary data associated with this article can be found in the online version at doi:10.1016/j.ydbio.2017.12.006.

References

Ahnfelt-Ronne, J., Ravassard, P., Pardanaud-Glavieux, C., Scharfmann, R., Serup, P., 2010. Mesenchymal bone morphogenetic protein signaling is required for normal pancreas development. Diabetes 59, 1948–1956.
Bertrand, J.Y., Chi, N.C., Santoso, B., Teng, S., Stainier, D.Y., Traver, D., 2010. Haematopoietic stem cells derive directly from aortic endothelium during development. Nature 464, 108–111.
Bhatia, M., Bonnet, D., Wu, D., Murdoch, B., Wrana, J., Gallacher, L., Dick, J.E., 1999. Bone morphogenetic proteins regulate the developmental program of human hematopoietic stem cells. J. Exp. Med. 189, 1139–1148.
Boisset, J.C., van Cappellen, W., Andrieu-Soler, C., Galjart, N., Dzierzak, E., Robin, C., 2010. In vivo imaging of haematopoietic cells emerging from the mouse aortic endothelium. Nature 464, 116–120.
de Bruijn, M., Ma, X., Robin, C., Ottersbach, K., Sanchez, M.J., Dzierzak, E., 2002. Hematopoietic stem cells localise to the endothelial cell layer in the midgestation mouse aorta. Immunity 16, 673–683.
Chadwick, K., Wang, L., Li, L., Menendez, P., Murdoch, B., Rouleau, A., Bhatia, M., 2003. Cytokines and BMP-4 promote hematopoietic differentiation of human embryonic stem cells. Blood 102, 906–915.
Chen, M.J., Yokomizo, T., Zeigler, B.M., Dzierzak, E., Speck, N.A., 2009. Runx1 is required for the endothelial to haematopoietic cell transition but not thereafter. Nature 457, 887–891.
Ciau-Uitz, A., Walmsley, M., Patient, R., 2000. Distinct origins of adult and embryonic blood in Xenopus. Cell 102, 787–796.
Crisan, M., Kartalaei, P.S., Vink, C.S., Yamada-Inagawa, T., Bollerot, K., van, I.W., van der Linden, R., de Sousa Lopes, S.M., Monteiro, R., Mummery, C., Dzierzak, E., 2015. BMP signalling differentially regulates distinct haematopoietic stem cell types. Nat. Commun. 6, 8040.
Crisan, M., Solaimani Kartalaei, P., Neagu, A., Karkanpouna, S., Yamada-Inagawa, T., Purini, C., Vink, C.S., van der Linden, R., van Ijcken, W., Chuva de Sousa Lopes, S.M., Monteiro, R., Mummery, C., Dzierzak, E., 2016. BMP and Hedgehog regulate distinct AGM hematopoietic stem cells Ex vivo. Stem Cell Rep. 6, 383–395.
Czechanski, A., Byers, C., Greenstein, I., Schrode, N., Donahue, L.R., Hadjantonakis, A.K., Reinholdt, L.G., 2014. Derivation and characterization of mouse embryonic stem cells from permissive and nonpermissive strains. Nat. Protoc. 9, 559–574.
Dang, S.M., Kyba, M., Perlingeiro, R., Daley, G.Q., Zandstra, P.W., 2002. Efficiency of embryoid body formation and hematopoietic development from embryonic stem cells in different culture systems. Biotechnol. Bioeng. 78, 442–453.
David, L., Mallet, C., Keramidas, M., Lamande, N., Gasc, J.M., Dupuis-Girod, S., Plauchu, H., Feige, J.J., Bailly, S., 2008. Bone morphogenetic protein-9 is a circulating vascular quiescence factor. Circ. Res. 102, 914–922.
Durand, C., Robin, C., Bollerot, K., Baron, M.H., Ottersbach, K., Dzierzak, E., 2007. Embryonic stromal clones reveal developmental regulators of definitive hematopoietic stem cells. Proc. Natl. Acad. Sci. USA 104, 20838–20843.
Dzierzak, E., Speck, N.A., 2008. Of lineage and legacy: the development of mammalian hematopoietic stem cells. Nat. Immunol. 9, 129–136.
Eilken, H.M., Nishikawa, S., Schroeder, T., 2009. Continuous single-cell imaging of blood generation from haemogenic endothelium. Nature 457, 896–900.
Faure, S., Barbara, de Santa, Roberts, P., Whitman, D.J., M, 2002. Endogenous patterns of BMP signaling during early chick development. Dev. Biol. 244, 44–65.
Finnson, K.W., Parker, W.L., Chi, Y., Hoemann, C.D., Goldring, M.B., Antoniou, J., Philip, A., 2010. Endoglin differentially regulates TGF-beta-induced Smad2/3 and Smad1/5 signalling and its expression correlates with extracellular matrix production and cellular differentiation state in human chondrocytes. Osteoarthr. Cartil. 18, 1518–1527.
Goossens, S., Janzen, V., Bartunkova, S., Yokomizo, T., Drogat, B., Crisan, M., Haigh, K., Seuntjens, E., Umans, L., Riedt, T., Bogaert, P., Haenebalcke, L., Berx, G., Dzierzak, E., Huylebroeck, D., Haigh, J.J., 2011. The EMT regulator Zeb2/Sip1 is essential for murine embryonic hematopoietic stem/progenitor cell differentiation and mobilization. Blood 117, 5620–5630.
Goumans, M.J., Valdimarsdottir, G., Itoh, S., Rosendahl, A., Sideras, P., ten Dijke, P., 2002. Balancing the activation state of the endothelium via two distinct TGF-beta type I receptors. EMBO J. 21, 1743–1753.
Hamburger, V., Hamilton, H.L., 1951. A series of normal stages in the development of the chick embryo. J. Morphol. 88, 49–92.
Huber, K., Franke, A., Bruhl, B., Krispin, S., Ernsberger, U., Schober, A., von Bohlen und Halbach, O., Rohrer, H., Kalcheim, C., Unsicker, K., 2008. Persistent expression of BMP-4 in embryonic chick adrenal cortical cells and its role in chromaffin cell development. Neural Dev. 3, 28.
Jaffredo, T., Gautier, R., Eichmann, A., Dieterlen-Lievre, F., 1998. Intraaortic hemopoietic cells are derived from endothelial cells during ontogeny. Development 125, 4575–4583.
Jaffredo, T., Gautier, R., Brajeul, V., Dieterlen-Lievre, F., 2000. Tracing the progeny of the aortic hemangioblast in the avian embryo. Dev. Biol. 224, 204–214.
James, D., Nam, H.S., Seandel, M., Nolan, D., Janovitz, T., Tomishima, M., Studer, L., Lee, G., Lyden, D., Benezra, R., Zaninovic, N., Rosenwaks, Z., Rabbany, S.Y., Rafii, S., 2010. Expansion and maintenance of human embryonic stem cell-derived endothelial cells by TGFbeta inhibition is Id1 dependent. Nat. Biotechnol. 28, 161–166.
Kalluri, R., Weinberg, R.A., 2009. The basics of epithelial-mesenchymal transition. J. Clin. Investig. 119, 1420–1428.
Kissa, K., Herbomel, P., 2010. Blood stem cells emerge from aortic endothelium by a novel type of cell transition. Nature 464, 112–115.
Knezevic, K., Bee, T., Wilson, N.K., Janes, M.E., Kinston, S., Polderdijk, S., Kolb-Kokocinski, A., Ottersbach, K., Pencovich, N., Groner, Y., de Bruijn, M., Gottgens, B., Pimanda, J.E., 2011. A Runx1-Smad6 rheostat controls Runx1 activity during embryonic hematopoiesis. Mol. Cell Biol. 31, 2817–2826.
Kume, T., 2010. Specification of arterial, venous, and lymphatic endothelial cells during embryonic development. Histol. Histopathol. 25, 637–646.
Lam, E.Y., Hall, C.J., Crosier, P.S., Crosier, K.E., Flores, M.V., 2010. Live imaging of Runx1 expression in the dorsal aorta tracks the emergence of blood progenitors from endothelial cells. Blood 116, 909–914.
Lamouille, S., Xu, J., Derynck, R., 2014. Molecular mechanisms of epithelial-mesenchymal transition. Nat. Rev. Mol. Cell Biol. 15, 178–196.
Lancrin, C., Sroczynska, P., Stephenson, C., Allen, T., Kouskoff, V., Lacaud, G., 2009. The haemangioblast generates haematopoietic cells through a haemogenic endothelium stage. Nature 457, 892–895.
Lebrin, F., Goumans, M.J., Jonker, L., Carvalho, R.L., Valdimarsdottir, G., Thorikay, M., Mummery, C., Arthur, H.M., ten Dijke, P., 2004. Endoglin promotes endothelial cell proliferation and TGF-beta/ALK1 signal transduction. EMBO J. 23, 4018–4028.
Lebrin, F., Deckers, M., Bertolino, P., Ten Dijke, P., 2005. TGF-beta receptor function in the endothelium. Cardiovasc. Res. 65, 599–608.
Li, N., Pasha, Z., Ashraf, M., 2014. Reversal of ischemic cardiomyopathy with Sca-1+ stem cells modified with multiple growth factors. PLoS One 9, e93645.
Liang, Y.Y., Brunicardi, F.C., Lin, X., 2009. Smad3 mediates immediate early induction of Id1 by TGF-beta. Cell Res. 19, 140–148.
Maeno, M., Mead, P.E., Kelley, C., Xu, R.H., Kung, H.F., Suzuki, A., Ueno, N., Zon, L.I., 1996. The role of BMP-4 and GATA-2 in the induction and differentiation of hematopoietic mesoderm in Xenopus laevis. Blood 88, 1965–1972.
Marshall, C.J., Kinnon, C., Thrasher, A.J., 2000. Polarized expression of bone morphogenetic protein-4 in the human aorta-gonad-mesonephros region. Blood 96, 1591–1593.
Medici, D., Kalluri, R., 2012. Endothelial-mesenchymal transition and its contribution to the emergence of stem cell phenotype. Semin. Cancer Biol. 22, 379–384.
Medvinsky, A., Dzierzak, E., 1996. Definitive hematopoiesis is autonomously initiated by the AGM region. Cell 86, 897–906.
Medvinsky, A., Rybtsov, S., Taoudi, S., 2011. Embryonic origin of the adult hematopoietic system: advances and questions. Development 138, 1017–1031.
Minko, K., Bollerot, K., Drevon, C., Hallais, M.F., Jaffredo, T., 2003. From mesoderm to blood islands: patterns of key molecules during yolk sac erythropoiesis. Gene Expr. Patterns 3, 261–272.
Miyazono, K., Kamiya, Y., Morikawa, M., 2010. Bone morphogenetic protein receptors and signal transduction. J. Biochem 147, 35–51.
Monteiro, R., Pinheiro, P., Joseph, N., Peterkin, T., Koth, J., Repapi, E., Bonkhofer, F., Kirmizitas, A., Patient, R., 2016. Transforming growth factor beta drives Hemogenic endothelium programming and the transition to hematopoietic stem cells. Dev. Cell 38, 358–370.
Monteiro, R.M., Lopes, de Sousa, Bialecka, S.M., de Boer, M., Zwijsen, S., Mummery, A., C.L, 2008. Real time monitoring of BMP Smads transcriptional activity during mouse development. Genesis 46, 335–346.
Müller, A.M., Medvinsky, A., Strouboulis, J., Grosveld, F., Dzierzak, E., 1994. Development of hematopoietic stem cell activity in the mouse embryo. Immunity 1, 291–301.
North, T., Gu, T.L., Stacy, T., Wang, Q., Howard, L., Binder, M., Marin-Padilla, M., Speck, N.A., 1999. Cbfa2 is required for the formation of intra-aortic hematopoietic clusters. Development 126, 2563–2575.
North, T.E., de Bruijn, M.F., Stacy, T., Talebian, L., Lind, E., Robin, C., Binder, M.,

Dzierzak, E., Speck, N.A., 2002. Runx1 expression marks long-term repopulating hematopoietic stem cells in the midgestation mouse embryo. Immunity 16, 661–672.
Oh, S.P., Seki, T., Goss, K.A., Imamura, T., Yi, Y., Donahoe, P.K., Li, L., Miyazono, K., ten Dijke, P., Kim, S., Li, E., 2000. Activin receptor-like kinase 1 modulates transforming growth factor-beta 1 signaling in the regulation of angiogenesis. Proc. Natl. Acad. Sci. USA 97, 2626–2631.
Pardali, E., Goumans, M.J., ten Dijke, P., 2010. Signaling by members of the TGF-beta family in vascular morphogenesis and disease. Trends Cell Biol. 20, 556–567.
Pimanda, J.E., Donaldson, I.J., de Bruijn, M.F., Kinston, S., Knezevic, K., Huckle, L., Piltz, S., Landry, J.R., Green, A.R., Tannahill, D., Gottgens, B., 2007. The SCL transcriptional network and BMP signaling pathway interact to regulate RUNX1 activity. Proc. Natl. Acad. Sci. USA 104, 840–845.
Reshef, R., Maroto, M., Lassar, A.B., 1998. Regulation of dorsal somitic cell fates: BMPs and Noggin control the timing and pattern of myogenic regulator expression. Genes Dev. 12, 290–303.
Richard, C., Drevon, C., Canto, P.Y., Villain, G., Bollerot, K., Lempereur, A., Teillet, M.A., Vincent, C., Rossello Castillo, C., Torres, M., Piwarzyk, E., Speck, N.A., Souyri, M., Jaffredo, T., 2013. Endothelio-Mesenchymal Interaction Controls runx1 Expression and Modulates the notch Pathway to Initiate Aortic Hematopoiesis. Dev. Cell 24, 600–611.
Rudini, N., Felici, A., Giampietro, C., Lampugnani, M., Corada, M., Swirsding, K., Garre, M., Liebner, S., Letarte, M., ten Dijke, P., Dejana, E., 2008. VE-cadherin is a critical endothelial regulator of TGF-beta signalling. EMBO J. 27, 993–1004.
Sela-Donenfeld, D., Kalcheim, C., 2002. Localized BMP4-noggin interactions generate the dynamic patterning of noggin expression in somites. Dev. Biol. 246, 311–328.
Shi, Y., Massague, J., 2003. Mechanisms of TGF-beta signaling from cell membrane to the nucleus. Cell 113, 685–700.
Sugiyama, D., Ogawa, M., Hirose, I., Jaffredo, T., Arai, K., Tsuji, K., 2003. Erythropoiesis from acetyl LDL incorporating endothelial cells at the preliver stage. Blood 101, 4733–4738.
Swiers, G., Baumann, C., O'Rourke, J., Giannoulatou, E., Taylor, S., Joshi, A., Moignard, V., Pina, C., Bee, T., Kokkaliaris, K.D., Yoshimoto, M., Yoder, M.C., Frampton, J., Schroeder, T., Enver, T., Gottgens, B., de Bruijn, M.F., 2013. Early dynamic fate changes in haemogenic endothelium characterized at the single-cell level. Nat. Commun. 4, 2924.
Taoudi, S., Medvinsky, A., 2007. Functional identification of the hematopoietic stem cell niche in the ventral domain of the embryonic dorsal aorta. Proc. Natl. Acad. Sci. USA 104, 9399–9403.
van Meeteren, L.A., ten Dijke, P., 2012. Regulation of endothelial cell plasticity by TGF-beta. Cell Tissue Res 347, 177–186.
Vargel, O., Zhang, Y., Kosim, K., Ganter, K., Foehr, S., Mardenborough, Y., Shvartsman, M., Enright, A.J., Krijgsveld, J., Lancrin, C., 2016. Activation of the TGFbeta pathway impairs endothelial to haematopoietic transition. Sci. Rep. 6, 21518.
Wagner, M., Siddiqui, M.A., 2009. Signaling networks regulating cardiac myocyte survival and death. Curr. Opin. Investig. Drugs 10, 928–937.
Walmsley, M., Ciau-Uitz, A., Patient, R., 2002. Adult and embryonic blood and endothelium derive from distinct precursor populations which are differentially programmed by BMP in Xenopus. Development 129, 5683–5695.
Watanabe, Y., Le Douarin, N.M., 1996. A role for BMP-4 in the development of subcutaneous cartilage. Mech. Dev. 57, 69–78.
Wilkinson, R.N., Pouget, C., Gering, M., Russell, A.J., Davies, S.G., Kimelman, D., Patient, R., 2009. Hedgehog and Bmp polarize hematopoietic stem cell emergence in the zebrafish dorsal aorta. Dev. Cell 16, 909–916.
Wilting, J., Eichmann, A., Christ, B., 1997. Expression of the avian VEGF receptor homologues Quek1 and Quek2 in blood-vascular and lymphatic endothelial and non-endothelial cells during quail embryonic development. Cell Tissue Res. 288, 207–223.
Yokomizo, T., Dzierzak, E., 2010. Three-dimensional cartography of hematopoietic clusters in the vasculature of whole mouse embryos. Development 137, 3651–3661.
Zhang, C., Lv, J., He, Q., Wang, S., Gao, Y., Meng, A., Yang, X., Liu, F., 2014. Inhibition of endothelial ERK signalling by Smad1/5 is essential for haematopoietic stem cell emergence. Nat. Commun. 5, 3431.
Zovein, A.C., Hofmann, J.J., Lynch, M., French, W.J., Turlo, K.A., Yang, Y., Becker, M.S., Zanetta, L., Dejana, E., Gasson, J.C., Tallquist, M.D., Iruela-Arispe, M.L., 2008. Fate tracing reveals the endothelial origin of hematopoietic stem cells. Cell Stem Cell 3, 625–636.